Bovine annulus fibrosus hydration affects rate-dependent failure mechanics in tension

Benjamin Werbner [a], Katherine Spack [a], Grace D. O'Connell [a,b,*]

[a] Department of Mechanical Engineering, University of California, Berkeley, United States
[b] Department of Orthopaedic Surgery, University of California, San Francisco, United States

ARTICLE INFO

ABSTRACT

The high water content of the intervertebral disc is essential to its load bearing function and viscoelastic mechanical behavior. One of the primary biochemical changes associated with disc degeneration is the loss of proteoglycans, which leads to tissue dehydration. While previous studies have reported the effects of *in vivo* degeneration on annulus fibrosus (AF) failure mechanics, the independent role of water remains unclear, as does the tissue's rate-dependent failure response. Our first objective was to determine the effect of loading rate on AF failure properties in tension; our second objective was to quantify the effect of water content on failure properties. Water content was altered through enzymatic digestion of glycosaminoglycans (GAGs) and through osmotic loading. Bovine AF specimens were tested monotonically to failure along the circumferential direction at 0.00697%/s or 6.97%/s. Increased loading rate resulted in a ~50% increase in linear-region modulus, failure stress, and strain energy density across all treatment groups (p < 0.001). Decreased GAG and water contents resulted in decreased modulus, failure stress, and strain energy density; however, these differences were only observed at the low loading rate (p < 0.05; no changes at high rate). Osmotic loading was used to evaluate the effect of hydration independently from GAG composition, resulting in similar decreases in water content, modulus, and strain energy density. This suggests that hydration is essential for maintaining tissue stiffness and energy absorption capacity, rather than strength, and that GAGs contribute to tissue strength independently from mediating water content.

1. Introduction

Back pain is a widespread public health concern, affecting millions of patients and incurring annual costs over $100 billion (Maniadakis and Gray, 2000; Katz, 2006). Back pain has been associated with degenerative changes in the intervertebral disc, including altered biochemical composition and an increase in annular tears (Buckwalter, 1995; Luoma et al., 2000; Urban and Roberts, 2003). Degeneration also has a significant effect on disc mechanical and rheological behavior (Maroudas et al., 1975; Adams et al., 1996). One of the most significant biochemical changes associated with degeneration is the fragmentation and loss of proteoglycans in the nucleus pulposus and inner annulus fibrosus (AF) (Lyons et al., 1981; Roughley et al., 2002). Proteoglycans are understood to be responsible for water absorption and retention through

osmotic pressure induced by negatively-charged glycosaminoglycans (GAGs) (Watanabe et al., 1998; Kiani et al., 2002). High tissue water content helps distribute compressive loads and contributes to the tissue's viscoelastic mechanical properties (Urban and Roberts, 2003; Iatridis et al., 2013). Thus, proteoglycan fragmentation and loss with degeneration is associated with tissue dehydration and loss of fluid support (Urban and McMullin, 1988; Adams et al., 1996).

In addition to these changes, previous studies have observed a multitude of structural and compositional changes with degeneration, making it difficult to discern the role of individual tissue constituents (Urban and Roberts, 2003; Adams and Roughley, 2006). Recent work by Isaacs *et al.* used enzymes to selectively digest individual molecules, isolating the role of each in tissue failure (Isaacs et al., 2014). However, such studies have typically only evaluated failure mechanics at one loading rate, making it difficult to elucidate the role of viscoelasticity on tissue failure (Green et al., 1993; Acaroglu et al., 1995; Isaacs et al., 2014). Furthermore, the authors of previous failure studies have consistently reported difficulties in ensuring failure occurred at a point away from the testing

---

* Corresponding author at: University of California, Berkeley, Department of Mechanical Engineering, 5122 Etcheverry Hall, #1740, Berkeley, CA 94720, United States.

E-mail address: g.oconnell@berkeley.edu (G.D. O'Connell).

grips, which may affect the reliability of the measured mechanics (Acaroglu et al., 1995; Ebara et al., 1996; Peloquin et al., 2016). Our previous work addressed this issue by developing a method to increase the likelihood of mid-substance failure during uniaxial tensile testing, significantly reducing variability in measured mechanical properties (Werbner et al., 2017).

Since GAG and water content affect the viscoelastic behavior of biological tissues, it is essential to consider potential rate-dependent effects of degeneration on disc failure properties (Elliott et al., 2003). Studies of similar fiber-reinforced tissues, such as tendons and ligaments, showed that failure stress and strain increased with loading rate (Noyes et al., 1974; Haut, 1983). Establishing similar structure-function relationships for the AF is important for understanding potential mechanisms of disc herniation (O'Connell et al., 2015). While several studies have investigated effects of degeneration and loading rate on AF sub-failure mechanics, the relationship between biochemical composition, loading rate, and AF failure mechanics is not yet well defined. With this in mind, the first objective of this study was to determine the effect of loading rate on AF tissue-level failure properties in uniaxial tension. The second objective was to quantify the effects of GAG and water content on AF failure mechanics.

2. Methods and materials

Nineteen caudal spine sections from adult bovines were acquired from a local abattoir. Bovine discs were used to investigate AF mechanics due to their larger disc area and similarities in biochemical and mechanical properties to healthy human discs (O'Connell et al., 2007; Demers et al., 2004; Beckstein et al., 2008). Musculature was removed from the spine and discs were dissected from levels C1-C4. Rectangular specimens approximately 2 mm thick were prepared from the middle-outer region of the anterior and posterior AF and oriented with the length along the circumferential direction and the width along the radial direction (n = 75; Fig. 1) (Werbner et al., 2017). This orientation was chosen in part for the greater contribution of the GAG-rich extrafibrillar matrix to the mechanical response (Holzapfel et al., 2005; O'Connell et al., 2009; Isaacs et al., 2014). Preliminary work ensured no differences in mechanics between anterior and posterior AF (n = 6/group, paired *t*-test p > 0.3).

Specimens were soaked in saline for 18 h at 37 °C prior to testing. Specimens in the control group (CTL group, n = 24) were soaked in 10 mL of phosphate-buffered saline (0.15 M PBS), while chondroitinase-treated specimens were soaked in 9.75 mL of saline with 0.25 mL of 10 U/mL chondroitinase ABC (chABC group, n = 26; enzyme concentration = 0.25 U/mL; Sigma-Aldrich, St. Louis, MO). To investigate the effect of water content independent of GAG content, specimens were soaked in a hyperosmotic saline solution (1.43 M NaCl, OSM group, n = 25).
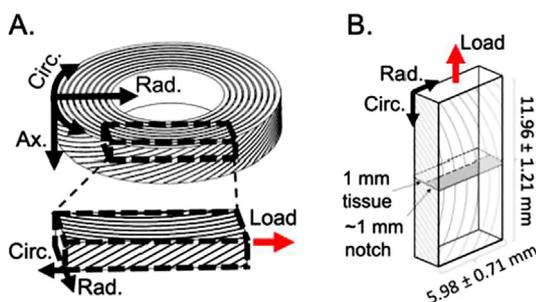

Fig. 1. (A) Schematic of circumferential-radial specimen orientation and direction of applied load. (B) Test specimen dimensions and notch geometry.
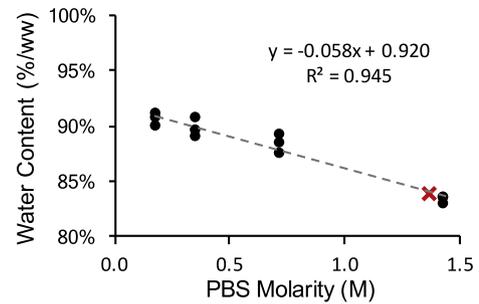

Fig. 2. Pearson correlation between PBS concentration and tissue water content after hydration (n = 12; black circles). The regression line was used to determine the PBS concentration needed to match tissue water content of chABC-treated samples (red 'X' = 1.43 M PBS). (For interpretation of the references to colour in this figure legend, the reader is referred to the web version of this article.)

Preliminary work determined the appropriate PBS concentration to match the reduced water content of chABC-treated specimens using osmotic loading. Twelve outer-middle AF biopsy punches were soaked in PBS solutions varying in concentration from 1.25 to 10 times greater than the control (n = 3 per concentration). Tissue weights were measured before and after soaking, and after lyophilization (Labconco 7740021, Kansas City, MO). Water content was calculated by dividing the difference between swollen (ww) and dry weights (dw) by the swollen weight (Eq. (1)). A Pearson correlation was performed to estimate the PBS concentration resulting in the observed chABC group water content (Fig. 2). Accordingly, OSM specimens were soaked in 1.43 M NaCl (~9.5X control concentration).

$$WC = (ww - dw)/ww \tag{1}$$

After soaking, specimens were trimmed using a parallel-block guide and razor blade to ensure uniform width (final width = 5.98 ± 0.71 mm). A full-width, half-depth notch was created to facilitate midlength failure (thickness at midlength = 1 mm) (Werbner et al., 2017). Several studies have reported no significant differences in stiffness or strength between notched and intact fiber-reinforced soft-tissue specimens, suggesting a limited effect of stress concentrations at the notch site (Taylor et al., 2012; Von Forell et al., 2014). Approximately 10% of the specimen length was glued into waterproof sandpaper; the final specimen length was 11.96 ± 1.21 mm. Samples were rehydrated in group-specific solutions for 30 min prior to testing. CTL and chABC samples were rehydrated in 0.15 M PBS, while OSM samples were rehydrated in 1.43 M PBS. Preliminary tests confirmed that the initial 18-hour treatment soak with 30 min of rehydration was sufficient to achieve steady-state hydration prior to testing (n = 6, Fig. S1). Specimens were tested in a custom-built water bath containing either 0.15 M PBS (CTL and chABC) or 1.43 M PBS (OSM).

Supplementary data associated with this article can be found, in the online version, at https://doi.org/10.1016/j.jbiomech.2019.04.008.

A monotonic 0.1 N preload was applied to remove slack from the tissue. Cyclic preconditioning was not applied to avoid altering pre-testing tissue water content, which could affect different treatment groups differently (Schmidt et al., 2016). Scale bar photographs were taken to measure sample-specific width and length. Uniaxial tension was applied monotonically along the circumferential direction at either a low or high loading rate until the specimen separated into two pieces (Low = 0.05 mm/min or 6.97×10^{-3}%/sec, High = 50 mm/min or 6.97%/sec). The large difference in loading rates was selected to be within the range of physiological loading conditions and to highlight relative differences, where quasi-static loading minimizes viscoelastic contributions from the tissue solid while facilitating fluid flow

and higher rate loading restricts fluid flow and emphasizes solid-component viscoelasticity. Applying uniaxial tension in the circumferential direction was intended to produce a failure mode representing AF failure by radial fissure.

Engineering strain was calculated as the measured change in displacement divided by the initial gauge length. Engineering stress was calculated as the measured force divided by the initial cross-sectional area at the midlength. Failure stress was defined as the maximum stress, and failure strain as the corresponding strain. The linear-region modulus was calculated using a linear-regression fit to the stress–strain response (Matlab Mathworks Inc.). Strain energy density was determined through numerical integration of the stress-strain response until failure.

After mechanical testing, a 4 mm biopsy punch was taken from the tissue midlength and specimen water content was determined as described above (Eq. (1)). Lyophilized samples were then digested in 2 mg/mL proteinase K. GAG content was determined using the 1,9-dimethylmethylene blue (DMMB) assay (Farndale et al., 1982). Solutions from the 18-hour tissue-soak were retained to measure GAGs in the solution, since previous studies reported GAG leaching from tissue during hydration (Urban and Maroudas, 1981; Han et al., 2012). Each tube of soak solution was centrifuged for 10 min at 5000 rpm and frozen before 72 h of lyophilization. Precipitates were digested in proteinase K and the DMMB assay used to determine GAG content. GAG content was normalized by both specimen dry and wet weights.

A two-way ANOVA was performed on mechanical and biochemical properties (factors = soak solution and loading rate). A Bonferroni post hoc analysis was performed where significance was found. Significance was assumed at $p < 0.05$. Values are reported as 'mean ± standard deviation.'

3. Results

All samples exhibited a nonlinear stress-strain response prior to failure (Fig. 3). A clear maximum stress, corresponding to the initiation of bulk failure, was observed for all specimens. Mechanical testing data was only analyzed for samples that clearly failed at the midlength (n = 66/75). For the low-rate control group (CTL-Low), the average linear-region modulus was 11.31 ± 1.75 MPa, strain energy density was 0.40 ± 0.16 MPa, failure stress was 2.25 ± 0.63 MPa, and failure strain was 0.36 ± 0.09 (Fig. 4 – light blue bars). Since loading rate did not significantly affect GAG or water content, biochemical data for both rates were pooled (p > 0.2). The average water content for the CTL group was 89.4 ± 5.9%. The average GAG content for controls was 0.98 ± 0.34%/ww normalized by swollen weight and 11.6 ± 5.0%/dw normalized by dry weight (Fig. 5 – blue bars).
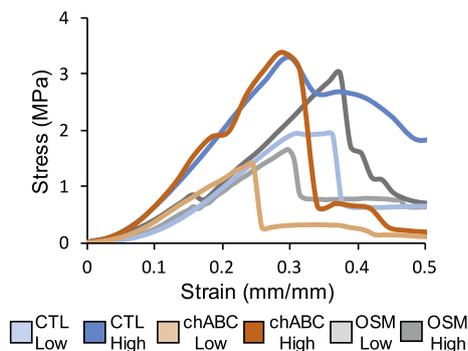
Fig. 3. Representative stress-strain curves showing one sample from each group. Each curve shows a non-linear sub-failure response, the point of failure, and post-failure behavior (data truncated at 50% strain for clarity).
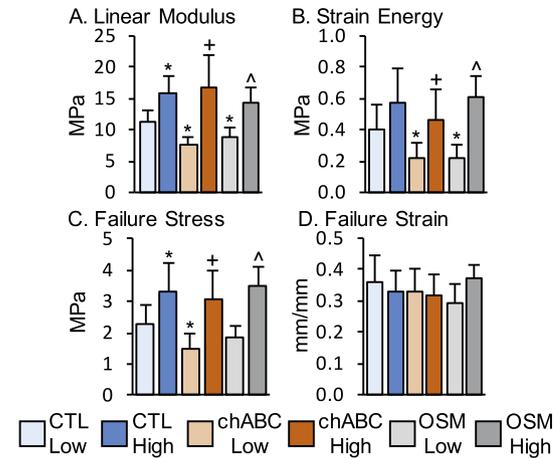
Fig. 4. Summary of mechanical properties in uniaxial tension (Mean + SD; n = 11 per group): (A) linear-region modulus, (B) strain energy density to the point of failure, (C) failure stress, and (D) failure strain. * denotes $p < 0.05$ vs CTL-Low, + denotes $p < 0.05$ vs chABC-Low, ^ denotes $p < 0.05$ vs OSM-Low in post-hoc analysis.

Loading rate had a significant effect on both sub-failure and failure properties, including linear-region modulus, strain energy density, and failure stress (all $p < 0.001$; Fig. 4 – dark vs light bars). The increase in loading rate resulted in a ~40% increase in linear-region modulus and a ~50% increase in failure stress (p < 0.03, CTL-Low vs CTL-High). Similarly, mechanical properties of chABC and OSM samples were dependent on loading rate, with significant increases in linear-region modulus, strain energy density, and failure stress (Fig. 4). Failure strain was not affected by loading rate for any treatment group (p > 0.2; Fig. 4D).

chABC treatment had a significant effect on mechanical and biochemical properties (Figs. 4 and 5 – blue vs orange bars). In particular, linear-region modulus, strain energy density, and failure stress were significantly affected by soak treatment (p < 0.05), as were water and GAG contents (p < 0.001). However, a post-hoc analysis showed that changes in mechanical properties with chABC treatment were only significant at the low loading rate (p > 0.2 for CTL-High vs chABC-High). At the lower loading rate, chABC treatment resulted in more than a 30% decrease in linear-region modulus and failure stress and a ~45% decrease in strain energy density (p < 0.04; Fig. 4). Failure strain was not affected by chABC treatment (p > 0.2; Fig. 4D). The post-hoc analysis also showed that water and GAG contents of chABC-treated samples were signifi-
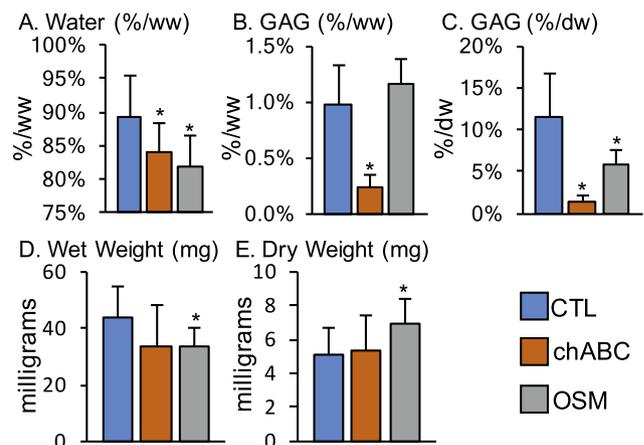
Fig. 5. Summary of biochemical data (Mean + SD; n = 22 per group): (A) water content normalized by swollen weight (ww), (B) GAG content normalized by swollen weight, (C) GAG content normalized by dry weight (dw), and (D) swollen and (E) dry weights of biopsy punches. Biochemical data from low- and high-rate loading groups were pooled. * denotes $p < 0.05$ vs CTL in post-hoc analysis.

cantly lower than the control. We observed a 6% decrease in water content in chABC samples compared to CTL (p < 0.001; chABC water content = 84%/ww; Fig. 5A), corresponding to a ∼85% decrease in GAG content (p < 0.001; chABC GAG content = 0.23 ± 0.12/ww or 1.46 ± 0.62%/dw; Fig. 5B–C).

Similar to chABC treatment, osmotic loading altered mechanical and biochemical properties, and significant differences were only observed at the lower loading rate (Figs. 4 and 5, blue vs grey bars). Osmotic loading resulted in a 22% decrease in linear-region modulus and a 44% decrease in strain energy density versus control (p < 0.04, CTL-Low vs OSM-Low). Failure stress and failure strain were not affected by osmotic loading (p > 0.2; Fig. 4). Water content was 7% lower in OSM samples compared to CTL (p < 0.001; Fig. 5A). There were no significant differences in GAG content when normalized by the swollen weight (p = 0.2; Fig. 5B), however GAG content normalized by dry weight was 50% lower than the control (p < 0.001; Fig. 5C).

Due to conflicting observations of GAG content in the OSM group, we directly compared swollen and dry weights of biopsy punches, assuming that punches had approximately equal tissue volumes. The average swollen weight of biopsy punches from OSM samples was significantly lower than those taken from CTL samples, as expected; however, the average dry weight of OSM specimens was greater than that of CTL specimens (p = 0.02; Fig. 5D-E). We also found that GAG content in the OSM soak solutions was not significantly different from that of the CTL soak solutions (p = 0.18).

4. Discussion

The overall aim of this study was to determine the effect of tissue water content on AF failure properties in tension. First, either low- or high-rate loading was applied independently to investigate differences in AF failure behavior under quasi-static and high-rate loading conditions. We employed a modified dog-bone geometry that ensured clear midlength failure in ∼90% of specimens. This represents a significant improvement in the failure testing of fiber-reinforced tissues with fibers oriented off-axis to the loading direction, where grip-line and mix-mode failures are commonly observed (Peloquin et al., 2016; Werbner et al., 2017). Second, we quantified the rate-dependent contribution of GAGs and water content to AF tensile behavior. Controlled GAG depletion was accomplished through enzymatic digestion using chondroitinase ABC. Since enzymatic degradation of GAGs lead to a decrease in water content, the independent effect of tissue hydration on failure behavior was investigated using osmotic loading. Finally, quantitative results regarding the effect of enzymatic digestion on AF GAG and water contents were assessed, since this data has not yet been provided in the literature.

An increase in loading rate significantly altered sub-failure and failure properties, including a ∼50% increase in linear-region modulus, strain energy density to failure, and failure stress. Increased moduli and failure stresses at higher loading rates were comparable in magnitude to those previously observed in viscoelastic tissues such as tendons. We believe that this observation is noteworthy considering the significant differences in tissue composition (e.g. GAG content) and subcomponent architecture (e.g. aligned vs off-axis fibers) (Noyes et al., 1974; Haut and Haut, 1997). Increased tissue strength and energy absorption capacity at high loading rates is essential for protecting against damage during sudden or unexpected loading; our results suggest that AF damage or rupture as a result of sudden, high-speed loads may be attributed to the disc experiencing greater forces during impact rather than the increased loading rate.

Viscoelastic properties of biological tissues were typically attributed to fluid flow (Mow et al., 1984); more recent studies, however, have also reported viscoelastic contributions from the solid matrix (Elliott et al., 2003; Zitnay and Weiss, 2018). AF specimens with depleted GAG and/or water contents were still highly sensitive to loading rate, with increases in sub-failure and failure properties that were comparable to or greater than the control (Fig. 4). Since similar increases in failure stress were observed for all treatment groups, the rate-dependent increase in failure stress was likely attributable to the collagen component of the solid matrix (i.e. non-GAG and non-water components). The relative increase in linear-region modulus with loading rate was greater for the chABC group than CTL (117% vs 40% increase), also suggesting significant collagen contribution to rate-dependent mechanics.

Samples with depleted GAG and/or water contents showed a significant decrease in both sub-failure and failure properties at the quasi-static loading rate, while no differences were observed at the higher rate. Our high-rate testing results were consistent with data from Isaacs et al. (2014) that reported no change in failure properties after chABC treatment. The lack of differences in mechanical properties between treatment groups at the high loading rate was likely due to restricted water flow during testing (Mow et al., 1984).

The primary mechanism of water retention in the AF is understood to be an osmotic gradient induced by negatively charged GAG molecules. Interestingly, our results showed that a ∼90% decrease in GAG content resulted in less than a 10% decrease in water content. Therefore, the tissue still retained high water content after GAG digestion (water content ∼80%/ww; Fig. 5), similar to previous observations in ligaments (Lujan et al., 2009). These findings suggest that GAGs are not the primary mechanism for water absorption and retention; it is possible that tissue permeability (AF permeability: $0.13–4.5 \times 10^{-15}$ m^4/Ns) and trapped intrafibrillar water may contribute to water retention more than was previously understood (Yao et al., 2002; Périé et al., 2005; Sivan et al., 2006; Schroeder et al., 2007). Similar mechanisms may also account for high water content of tendons and ligaments despite their low GAG content (water content >65%, GAG content <5%) (Yoon and Halper, 2005; Lujan et al., 2009).

Mechanical properties and GAG content of the control group were consistent with results previously reported for human and bovine AF (Acaroglu et al., 1995; Ebara et al., 1996; Demers et al., 2004). The decrease in linear-region modulus observed with osmotic loading was contrary to data presented for specimens oriented along the circumferential-axial direction (Han et al., 2012). This discrepancy was likely due to greater collagen fiber engagement in circumferential-axial specimens, whereas the response from circumferential-radial specimens was dominated by the extra-fibrillar matrix (Holzapfel et al., 2005; O'Connell et al., 2009). This suggests that structural anisotropy may play an important role in tissue failure properties with respect to hydration.

chABC treatment has been widely used to decrease both GAG and water contents, while osmotic loading has been used to alter hydration levels without changing tissue composition (Bezci and O'Connell, 2018). Previous work by Han et al. (2012) observed a decrease in tissue GAG content (normalized by dry weight) after osmotic loading. Unlike the current study, Han et al. (2012) did not observe significant changes in tissue dry weight; therefore, the decrease in GAG content was attributed to GAGs leaching into the surrounding solution. In this study, GAGs in the soak solution were measured and no significant differences were observed between CTL and OSM groups (p = 0.2). Moreover, GAG content normalized by wet weight showed no significant differences between CTL and OSM. Together, these results suggest that the apparent decrease in GAG content with osmotic loading may be an artifact caused by salt migration into or onto the tissue, increasing tissue density and resulting in a lower apparent GAG content with respect to dry weight. These findings highlight the impor-

tance of normalizing biochemical results by both wet and dry weights.

One limitation of this study was our choice to free-swell tissue specimens before mechanical testing, as tissue mechanics are known to change with hydration (Bezci and O'Connell, 2018). While this resulted in water contents that were greater than values typically reported in the literature, this procedure was chosen to best suit our aims and experimental design; the extended hydration period was largely driven by our GAG depletion protocol, which required 18 h of submersion in an enzyme solution. A more complete understanding of diurnal changes of *in vivo* water content is required to extrapolate the findings of the current study for clinical purposes; however, joint-level testing and clinical observations suggest that tissue hydration does alter disc mechanics and the risk of spinal injury (Adams et al., 1987; Adams et al., 1990; Belavy et al., 2016). An additional limitation of this study is that only circumferential-radial specimens were tested, where the mechanical contribution of collagen fibers is limited. This orientation was chosen to represent AF failure by radial fissure, which, in addition to circumferential delamination, has been associated with disc bulging and lower back pain (Veres et al., 2008; Tavakoli et al., 2018; Buirski, 1992).

The current study provides new insights into the structure-function relationship between AF water content and tensile mechanics. Decreases in GAG and water content corresponded with decreases in tissue stiffness, strength, and strain energy density. Osmotic loading resulted in similar decreases in stiffness, strain energy density, and water content. In conclusion, these results suggest that tissue hydration is essential for maintaining bulk tissue stiffness and capacity for energy absorption, rather than strength. Moreover, hydration altered tissue stiffness and strength at the quasi-static loading rate, where fluid flows more freely, but not at the higher loading rate. This suggests that viscoelasticity of the extrafibrillar matrix plays an important role in stress distribution between fibers and the resistance to bulk tissue failure. These findings are important for defining design criterion for biological repair strategies that recapitulate the behavior of healthy native tissues and for understanding mechanisms of annular tears with injury and degeneration.

Acknowledgements

Conflict of interest statement

The authors have no Conflicts of Interest to disclose.

References

Acaroglu, E.R., Iatridis, J.C., Setton, L.A., Foster, R.J., Mow, V.C., Weidenbaum, M., 1995. Degeneration and aging affect the tensile behavior of human lumbar anulus fibrosus. Spine 20 (24), 2690–2701.

Adams, M.A., Dolan, P., Hutton, W.C., 1987. Diurnal variations in the stresses on the lumbar spine. Spine 12 (2), 130–137.

Adams, M.A., Dolan, P., Hutton, W.C., Porter, R.W., 1990. Diurnal changes in spinal mechanics and their clinical significance. J. Bone Joint Surg. British volume. 72 (2), 266–270.

Adams, M.A., McNally, D.S., Dolan, P., 1996. 'Stress' distributions inside intervertebral discs: the effects of age and degeneration. J. Bone Joint Surg. British volume. 78 (6), 965–972.

Adams, M.A., Roughley, P.J., 2006. What is intervertebral disc degeneration, and what causes it? Spine 31 (18), 2151–2161.

Beckstein, J.C., Sen, S., Schaer, T.P., Vresilovic, E.J., Elliott, D.M., 2008. Comparison of animal discs used in disc research to human lumbar disc: axial compression mechanics and glycosaminoglycan content. Spine 33 (6), E166–E173.

Belavy, D.L., Adams, M., Brisby, H., Cagnie, B., Danneels, L., Fairbank, J., Hargens, A.R., Judex, S., Scheuring, R.A., Sovelius, R., Urban, J., 2016. Disc herniations in astronauts: what causes them, and what does it tell us about herniation on earth? Eur. Spine J. 25 (1), 144–154.

Bezci, S.E., O'Connell, G.D., 2018. Osmotic pressure alters time-dependent recovery behavior of the intervertebral disc. Spine. 43 (6), E334–E340.

Buckwalter, J.A., 1995. Aging and degeneration of the human intervertebral disc. Spine 20 (11), 1307–1314.

Buirski, G., 1992. Magnetic resonance signal patterns of lumbar discs in patients with low back pain. A prospective study with discographic correlation. Spine 17 (10), 1199–1204.

Demers, C.N., Antoniou, J., Mwale, F., 2004. Value and limitations of using the bovine tail as a model for the human lumbar spine. Spine 29 (24), 2793–2799.

Ebara, S., Iatridis, J.C., Setton, L.A., Foster, R.J., Mow, V.C., Weidenbaum, M., 1996. Tensile properties of nondegenerate human lumbar anulus fibrosus. Spine 21 (4), 452–461.

Elliott, D.M., Robinson, P.S., Gimbel, J.A., Sarver, J.J., Abboud, J.A., Iozzo, R.V., Soslowsky, L.J., 2003. Effect of altered matrix proteins on quasilinear viscoelastic properties in transgenic mouse tail tendons. Ann. Biomed. Eng. 31 (5), 599–605.

Farndale, R.W., Sayers, C.A., Barrett, A.J., 1982. A direct spectrophotometric microassay for sulfated glycosaminoglycans in cartilage cultures. Connect. Tissue Res. 9 (4), 247–248.

Green, T.P., Adams, M.A., Dolan, P., 1993. Tensile properties of the annulus fibrosus. Eur. Spine J. 2 (4), 209–214.

Han, W.M., Nerurkar, N.L., Smith, L.J., Jacobs, N.T., Mauck, R.L., Elliott, D.M., 2012. Multi-scale structural and tensile mechanical response of annulus fibrosus to osmotic loading. Ann. Biomed. Eng. 40 (7), 1610–1621.

Haut, R.C., 1983. Age-dependent influence of strain rate on the tensile failure of rat-tail tendon. J. Biomech. Eng. 105 (3), 296–299.

Haut, T.L., Haut, R.C., 1997. The state of tissue hydration determines the strain-rate-sensitive stiffness of human patellar tendon. J. Biomech. 30 (1), 79–81.

Holzapfel, G.A., Schulze-Bauer, C.A., Feigl, G., Regitnig, P., 2005. Single lamellar mechanics of the human lumbar anulus fibrosus. Biomech. Modeling Mechanobiol. 3 (3), 125–140.

Iatridis, J.C., Nicoll, S.B., Michalek, A.J., Walter, B.A., Gupta, M.S., 2013. Role of biomechanics in intervertebral disc degeneration and regenerative therapies: what needs repairing in the disc and what are promising biomaterials for its repair? Spine J. 13 (3), 243–262.

Isaacs, J.L., Vresilovic, E., Sarkar, S., Marcolongo, M., 2014. Role of biomolecules on annulus fibrosus micromechanics: Effect of enzymatic digestion on elastic and failure properties. J. Mech. Behav. Biomed. Mater. 1 (40), 75–84.

Katz, J.N., 2006. Lumbar disc disorders and low-back pain: socioeconomic factors and consequences. J. Bone Joint Surg. 1 (88), 21–24.

Kiani, C., Liwen, C.H., Wu, Y.J., Albert, J.Y., Burton, B.Y., 2002. Structure and function of aggrecan. Cell Res. 12 (1), 19.

Lujan, T.J., Underwood, C.J., Jacobs, N.T., Weiss, J.A., 2009. Contribution of glycosaminoglycans to viscoelastic tensile behavior of human ligament. J. Appl. Physiol. 106 (2), 423–431.

Luoma, K., Riihimäki, H., Luukkonen, R., Raininko, R., Viikari-Juntura, E., Lamminen, A., 2000. Low back pain in relation to lumbar disc degeneration. Spine. 25 (4), 487–492.

Lyons, G., Eisenstein, S.M., Sweet, M.B., 1981. Biochemical changes in intervertebral disc degeneration. Biochimica et Biophysica Acta - General Subjects. 1 (673), 443–453.

Maniadakis, N., Gray, A., 2000. The economic burden of back pain in the UK. Pain 84 (1), 95–103.

Maroudas, A., Stockwell, R.A., Nachemson, A., Urban, J., 1975. Factors involved in the nutrition of the human intervertebral disc: cellularity and diffusion of glucose in vitro. J. Anat. 120 (Pt 1), 113.

Mow, V.C., Holmes, M.H., Lai, W.M., 1984. Fluid transport and mechanical properties of articular cartilage: a review. J. Biomech. 17 (5), 377–394.

Noyes, F.R., DeLucas, J.L., Torvik, P.J., 1974. Biomechanics of anterior cruciate ligament failure: an analysis of strain-rate sensitivity and mechanisms of failure in primates. J. Bone Joint Surg. 56, 236–253.

O'Connell, G.D., Leach, J.K., Klineberg, E.O., 2015. Tissue engineering a biological repair strategy for lumbar disc herniation. BioResearch Open Access. 4 (1), 431–445.

O'Connell, G.D., Guerin, H.L., Elliott, D.M., 2009. Theoretical and uniaxial experimental evaluation of human annulus fibrosus degeneration. J. Biomech. Eng. 131, (11) 111007.

O'Connell, G.D., Vresilovic, E.J., Elliott, D.M., 2007. Comparison of animals used in disc research to human lumbar disc geometry. Spine 32 (3), 328–333.

Peloquin, J.M., Santare, M.H., Elliott, D.M., 2016. Advances in quantification of meniscus tensile mechanics including nonlinearity, yield, and failure. J. Biomech. Eng. 138, (2) 021002.

Périé, D., Korda, D., Iatridis, J.C., 2005. Confined compression experiments on bovine nucleus pulposus and annulus fibrosus: sensitivity of the experiment in the determination of compressive modulus and hydraulic permeability. J. Biomech. 38 (11), 2164–2171.

Roughley, P.J., Alini, M., Antoniou, J., 2002. The role of proteoglycans in aging, degeneration and repair of the intervertebral disc. Biochem. Soc. Trans. 30 (6).

Schmidt, H., Schilling, C., Reyna, A.L., Shirazi-Adl, A., Dreischarf, M., 2016. Fluid-flow dependent response of intervertebral discs under cyclic loading: on the role of specimen preparation and preconditioning. J. Biomech. 49 (6), 846–856.

Schroeder, Y., Sivan, S., Wilson, W., Merkher, Y., Huyghe, J.M., Maroudas, A., Baaijens, F.P., 2007. Are disc pressure, stress, and osmolarity affected by intra- and extrafibrillar fluid exchange? J. Orthop. Res. 25 (10), 1317–1324.

Sivan, S., Merkher, Y., Wachtel, E., Ehrlich, S., Maroudas, A., 2006. Correlation of swelling pressure and intrafibrillar water in young and aged human intervertebral discs. J. Orthop. Res. 24 (6), 1292–1298.

Tavakoli, J., Amin, D.B., Freeman, B.J., Costi, J.J., 2018. The biomechanics of the inter-lamellar matrix and the lamellae during progression to lumbar disc herniation: which is the weakest structure? Ann. Biomed. Eng. 21, 1–2.

Taylor, D., O'Mara, N., Ryan, E., Takaza, M., Simms, C., 2012. The fracture toughness of soft tissues. J. Mech. Behav. Biomed. Mater. 1 (6), 139–147.

Urban, J.P., Maroudas, A., 1981. Swelling of the intervertebral disc in vitro. Connect. Tissue Res. 9 (1), 1.

Urban, J.P., McMullin, J.F., 1988. Swelling pressure of the lumbar intervertebral discs: influence of age, spinal level, composition, and degeneration. Spine 13 (2), 179–187.

Urban, J.P., Roberts, S., 2003. Degeneration of the intervertebral disc. Arthritis Res. Therapy 5 (3), 120.

Veres, S.P., Robertson, P.A., Broom, N.D., 2008. ISSLS prize winner: microstructure and mechanical disruption of the lumbar disc annulus: part II: how the annulus fails under hydrostatic pressure. Spine 33 (25), 2711–2720.

Von Forell, G.A., Hyoung, P.S., Bowden, A.E., 2014. Directional failure of tendons in the presence of a notch defect. Mech. Biol. Syst. Mater. 4, 11–14.

Watanabe, H., Yamada, Y., Kimata, K., 1998. Roles of aggrecan, a large chondroitin sulfate proteoglycan, in cartilage structure and function. J. Biochem. 124 (4), 687–693.

Werbner, B., Zhou, M., O'Connell, G., 2017. A novel method for repeatable failure testing of annulus fibrosus. J. Biomech. Eng. 139, (11) 111001.

Yao, H., Justiz, M.A., Flagler, D., Gu, W.Y., 2002. Effects of swelling pressure and hydraulic permeability on dynamic compressive behavior of lumbar annulus fibrosus. Ann. Biomed. Eng. 30 (10), 1234–1241.

Yoon, J.H., Halper, J., 2005. Tendon proteoglycans: biochemistry and function. J. Musculoskelet. Neuronal Interact. 5 (1), 22–34.

Zitnay, J.L., Weiss, J.A., 2018. Load transfer, damage and failure in ligaments and tendons. J. Orthop. Res. Sep 3.